Stem Cells, 2026, **44**, sxag057
https://doi.org/10.1093/stmcls/sxag057
Published: October 12, 2026
Brief Report

OXFORD

Paracrine bone-derived senescent secretome is associated with spatially patterned extracellular matrix remodeling and altered biomechanics in human brain organoids

Chanul Kim[1], Luke D. Ofria[2], Hossein Shaygani[3], Anannya Kshirsagar[2], Sai Kulkarni[2], Alan Y. Liu[4], James L. Kirkland[5], Annie Kathuria[*,2], Maryam Tilton[*,3]

[1]Department of Biomedical Engineering, The University of Texas at Austin, Austin, TX 78712, United States
[2]Department of Biomedical Engineering, Johns Hopkins University, Baltimore, MD 21205, United States
[3]Walker Department of Mechanical Engineering, The University of Texas at Austin, Austin, TX 78712, United States
[4]Optics11 Life Inc., Boston, MA 02111, United States
[5]Center for Advanced Gerotherapeutics, Division of Endocrinology, Department of Medicine, Cedars-Sinai Medical Center, Los Angeles, CA 90048, United States
*Corresponding authors: Maryam Tilton, Walker Department of Mechanical Engineering, The University of Texas at Austin, 204 E. Dean Keeton St., RM 4.138, Austin, TX 78712, USA. E-mail: maryam.tilton@austin.utexas.edu; Annie Kathuria, Department of Biomedical Engineering, Johns Hopkins University, 720 Rutland Ave., Smith 6029, Baltimore, MD 21205, USA. E-mail: annie_kathuria@jhu.edu.

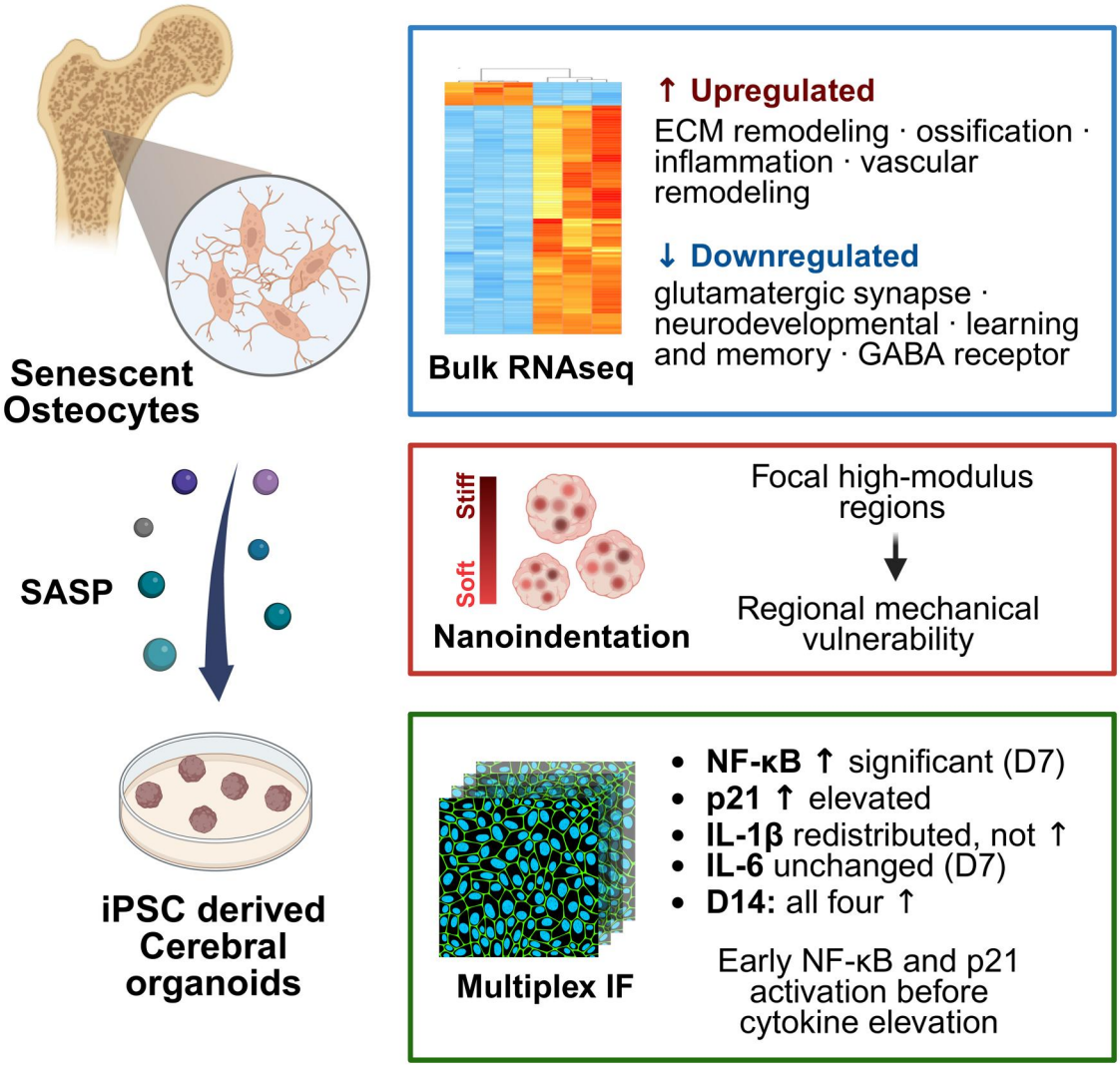
Abstract

Aging is increasingly recognized as a systemic process, yet the mechanisms by which signals from senescent peripheral cells accelerate brain aging remain poorly defined. Here, we used chronic exposure of human cerebral organoids to the secretome of senescent osteocytes to investigate how peripheral aging signals from bone reshape brain tissue architecture. We combined spatially resolved optical fiber-based interferometry nanoindentation with transcriptomic and immunofluorescence profiling, revealing distinct mechanical features across complementary measurements, including lower apparent modulus in intact organoids and spatially localized regions of elevated modulus in cryosectioned specimens. This spatially heterogeneous biomechanical remodeling was accompanied by upregulation of extracellular matrix (ECM), inflammatory, and senescence pathways, and suppression of neurodevelopmental and synaptic gene networks. Our results suggest that chronic paracrine exposure to senescent osteocyte-derived secretome is associated with localized extracellular matrix-related remodeling and mechanical vulnerability in human brain tissue, providing insight into how peripheral cellular senescence may contribute to regional brain fragility during aging. These pilot-scale findings were obtained using a single induced pluripotent stem cell line and a single conditioned-medium batch, with 1-6 experimental replicates per condition across assays; the mechanical analyses were exploratory.

Key words: bone-brain axis; cellular senescence; paracrine signaling; neuroinflammation; biomechanical remodeling

Received: April 28, 2026. **Accepted:** September 29, 2026
© The Author(s) 2026. Published by Oxford University Press.
This is an Open Access article distributed under the terms of the Creative Commons Attribution-NonCommercial License (https://creativecommons.org/licenses/by-nc/4.0/), which permits non-commercial re-use, distribution, and reproduction in any medium, provided the original work is properly cited. For commercial re-use, please contact reprints@oup.com for reprints and translation rights for reprints. All other permissions can be obtained through our RightsLink service via the Permissions link on the article page on our site—for further information please contact journals.permissions@oup.com.

Graphical abstract



Significance statement

This study investigates how senescence-associated signals from bone may influence the brain, focusing on their effects on tissue organization, mechanics, and early inflammatory and senescence-associated signaling. Using a cross-organ human organoid model, we found that bone-derived senescence-associated secretory phenotype exposure was associated with localized structural disruption and spatially heterogeneous mechanical vulnerability in cerebral tissue. These findings suggest that senescent bone-derived signals may contribute to region-specific brain fragility before overt neurodegenerative manifestations, offering a new framework for understanding bone-brain comorbidities in aging.

Introduction

Aging is a major risk factor for both neurodegenerative diseases and musculoskeletal deterioration.[1] Studies indicate that individuals over the age of 65 with bone loss have a higher risk of developing dementia.[1] Since the economic burden of neurodegeneration is projected to reach $1.5 trillion by 2050 and bone loss costs are expected to rise to $95 billion in the United States,[2] understanding the mechanistic links between bone health and brain aging has become an urgent public health priority.[1] Emerging research suggests that bone and brain aging share common molecular drivers, including chronic inflammation, oxidative stress, and cellular senescence,[3] highlighting the need to study the "bone-brain axis" holistically.

One key mechanism linking bone aging to brain dysfunction is cellular senescence.[3] Senescent bone cells, including osteocytes

and bone marrow stromal cells, accumulate with age and secrete a pro-inflammatory, tissue-remodeling secretome known as the senescence-associated secretory phenotype (SASP). In parallel, osteocytes release bone-derived signaling molecules with systemic activity. Notably, osteocyte-derived sclerostin has been shown to cross the blood-brain barrier (BBB) in aged mice and impair synaptic plasticity and memory.[4–6] However, whether and to what extent components of the senescent osteocyte secretome access brain parenchyma in vivo remain incompletely defined. Yet, cross-organ signals, reflected in mitochondrial deficits, proteostasis decline, and chronic inflammation, are shared features of aged cells across organs. Furthermore, preclinical studies show that youthful bone-derived factors can enhance memory and systemic rejuvenation,[7,8] underscoring the potential for bone-secreted molecules to modulate brain function. Brain aging can be accompanied by remodeling of the extracellular matrix and altered tissue mechanical properties, which can influence cellular organization, neuronal and glial behavior, and the local signaling environment.[9] We therefore consider spatial mechanical changes as a tissue-level readout of microenvironmental remodeling rather than a surrogate for cognitive function.

Here, we developed a cross-organ aging model in which patient-derived cerebral organoids were exposed to SASP-enriched conditioned media from irradiation-induced senescent osteocytes using our previously validated single 10-Gy dose protocol.[10,11] Because this design bypasses the circulation and BBB, it isolates the cerebral tissue response to osteocyte-derived senescence signals rather than their systemic transport or brain entry in vivo. Using longitudinal micromechanical profiling, live-cell quantitative imaging, transcriptomics, and immunofluorescence, we examined whether exposure to the senescent osteocyte secretome is associated with changes in organoid biomechanics, inflammatory signaling, and aging-associated molecular programs. This platform therefore provides a human experimental framework for interrogating recipient-tissue responses within the bone-brain axis. To our knowledge, this study is among the first to associate osteocyte-derived senescent secretomes with neuroinflammatory and aging-associated biomechanical and molecular remodeling in human cerebral organoids.

Methods

Preparation and validation of senescent osteocyte-conditioned medium

Senescent osteocyte-conditioned medium (SASP-CM) was generated using MLO-Y4 osteocyte cultures, as previously described and validated by our team.[10] Details are provided in Supplementary Material: S1, Figure S1 (see online supplementary material for a color version of this figure).

Cerebral organoid generation and treatment

Cerebral organoids were generated from induced pluripotent stem cells (iPSCs) using a guided neural differentiation protocol with Matrigel embedding to support three-dimensional tissue organization. Organoids were cultured for 60 days of differentiation prior to experimentation; single-nucleus RNA-seq at this stage confirmed the presence of diverse neuronal and nonneuronal populations characteristic of developing cerebral tissue (Supplementary Material S9, Figure S2, see online supplementary material for a color version of this figure). Organoids were then randomly divided into 2 groups: (1) a control group, for which the medium was changed to α-Minimum Essential Medium Eagle (αMEM) supplemented with 5% fetal bovine serum, 5% calf serum, and 1% penicillin-streptomycin (10 000 U mL^{-1}) (Table S1); and (2) a SASP-CM group, for which the medium was changed to osteocyte-derived SASP-CM prepared in the same complete αMEM background media (Figure 1A). Organoids from both study groups were collected on days 7 and 14 posttreatment for downstream analyses (Supplementary Material).

Biomechanical remodeling of cerebral organoids following SASP exposure

Nanoindentation testing was performed on both live intact cerebral organoids and 20-μm thick cryosectioned slices using an optical fiber-based interferometry nanoindenter. Indentations were performed in Peak Load Poking across a 50 μm × 50 μm grid (Table S2). The apparent Young's modulus for sample types was calculated using Hertzian contact mechanics to assess local tissue mechanical properties, while the Dimitriadis model[12] was additionally applied to sectioned samples to account for finite sample thickness effects. Indentation force-displacement curves were analyzed using DataViewer (Optics11 Life).

In vitro cerebral organoid assays

Detailed protocols for live/dead staining, immunofluorescence analysis, and SASP transcriptomic profiling are described in Supplementary Material: S4-S7 and S9.

Ethics approval and informed consent

The human iPSC line MH0185984 was obtained from the NIMH Repository & Genomics Resource and was used as an established repository-derived cell line. No new human participants were recruited or biospecimens collected for this study; therefore, separate institutional ethics approval was not required for the present work.

Statistical analyses

All statistical analyses were performed in GraphPad Prism and Python (for further details on the statistical analyses used, see Supplementary Material: S6, S8, and S9).

Results

Bone-derived SASP exposure induced subtle but progressive cytoskeletal and viability alterations in cerebral organoids

To document organoid viability and cytoskeletal organization following paracrine exposure to bone-derived senescent

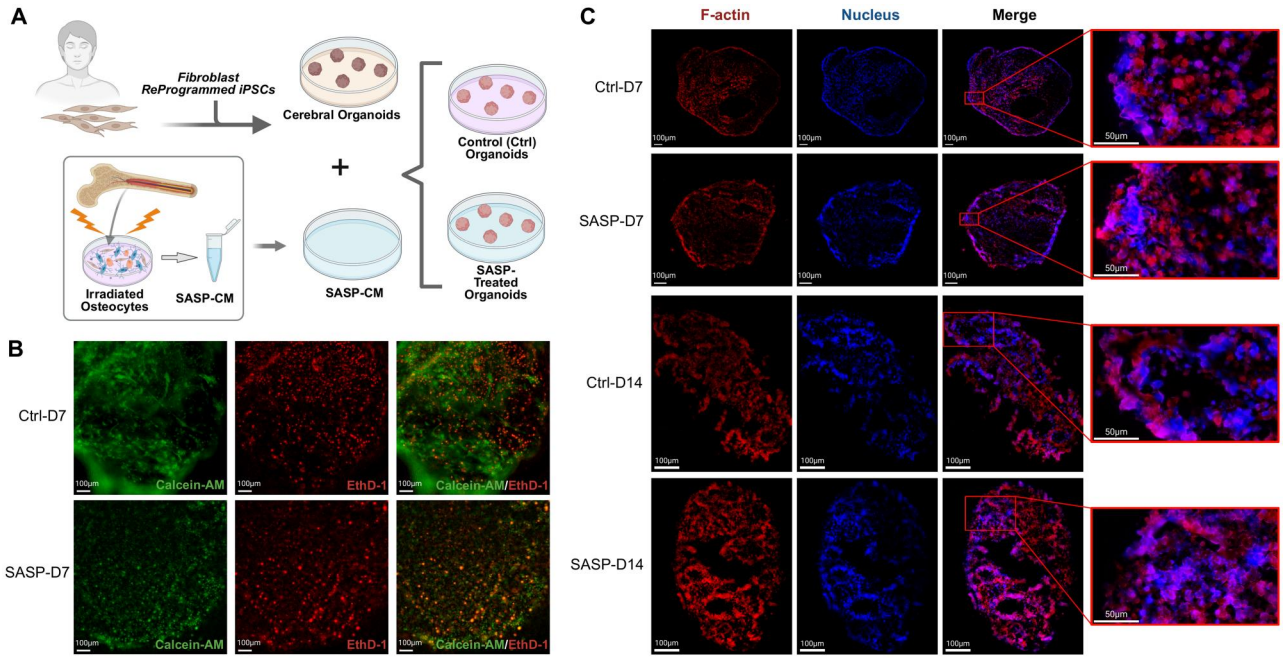


Figure 1. Bone-derived SASP alters structure and cytoskeletal organization in cerebral organoids. (A) Experimental workflow: iPSC-derived cerebral organoids cultured with or without SASP-CM. (B) Live/dead staining of D7 control and SASP-treated organoids. Calcein AM (viability); Ethidium homodimer-1 (loss of membrane integrity, dead cells). Scale bar = 100 μm. (C) Immunofluorescence of F-actin and nuclei across groups. CellMask Deep Red (F-actin, cytoskeletal organization); DAPI (nuclei). Scale bar = 100 μm (overview) and 50 μm (magnified). Live/dead: $n = 1$ (Ctrl-D7) and 5 (SASP-D7). F-actin: $n = 3$ (Ctrl-D7), 2 (SASP-D7), 3 (Ctrl-D14), and 6 (SASP-D14). Representative images shown. Abbreviations: iPSC, induced pluripotent stem cell; SASP, senescence-associated secretory phenotype. Created in BioRender. Kim, C. (2026) https://BioRender.com/9m772ux

secretomes, live/dead staining and F-actin imaging were performed (Figure 1B and C). These analyses were qualitative and were not designed for quantitative comparison between groups. Live/dead imaging at D7 (Figure 1B) showed high overall viability and modest EthD-1 signal in both groups, with interior EthD-1-positive clusters observed in all 5 SASP-exposed specimens, although the extent varied among specimens. Cytoskeletal imaging (Figure 1C) showed peripheral F-actin organization at D7 and a denser, more spatially compact actin architecture at D14 in specimens from both groups.

Bone-derived SASP exposure is associated with altered mechanical properties in cerebral organoids

To examine the mechanobiological consequences of SASP exposure, we performed optical fiber-based interferometry nanoindentation (Figure 2A), combining nondestructive testing of intact live organoids with localized mechanophenotyping of cryosectioned specimens to resolve bulk mechanical changes and spatial single-cell heterogeneity following exposure to bone-derived SASP.

Nanoindentation of intact live organoids (Figure 2B) showed higher apparent moduli in control samples at D14 than D7, increasing from ∼188 to ∼484 Pa, consistent with culture-associated bulk mechanical maturation and tissue-level consolidation. In contrast, SASP-exposed organoids showed lower values at both time points (∼72 Pa at D7 and ∼142 Pa at D14). Given the limited organoid-level replication ($n = 1$-3 per condition), these measurements are presented as exploratory observations rather than inferential group comparisons (Supplementary Material S6a).

Cryosection-based nanoindentation provided higher-resolution insight into local mechanical organization (Figure 2C-i and C-ii). Mean apparent modulus values were ∼35.1, ∼56.6, ∼9.9, and ∼47.9 kPa for Ctrl-D7, SASP-D7, Ctrl-D14, and SASP-D14, respectively. Exploratory replicate-level analysis identified significant differences between Ctrl-D14 and SASP-D14, and between SASP-D7 and Ctrl-D14; all other pairwise comparisons were not significant (Supplementary Material S6b). Spatial stiffness maps further illustrated focal high-modulus regions within SASP-exposed sections. These measurements comprise $n = 2$, 2, 2, and 5 experimental replicates for Ctrl-D7, SASP-D7, Ctrl-D14, and SASP-D14, respectively, and the accompanying analyses are reported as exploratory. These data suggest that SASP exposure is associated with altered apparent mechanical properties in intact organoids.

Bone-derived SASP induces pro-inflammatory transcriptional response in cerebral organoids

To define early transcriptional responses to bone-derived SASP exposure, bulk RNA sequencing was performed on D7 organoids, addressing a largely uncharacterized aspect of aging despite systemic inflammation being a hallmark.[13] Differential gene expression and pathway enrichment analysis revealed inflammatory and aging-associated programs induced by chronic SASP exposure, implicating the role of senescent bone cells in brain

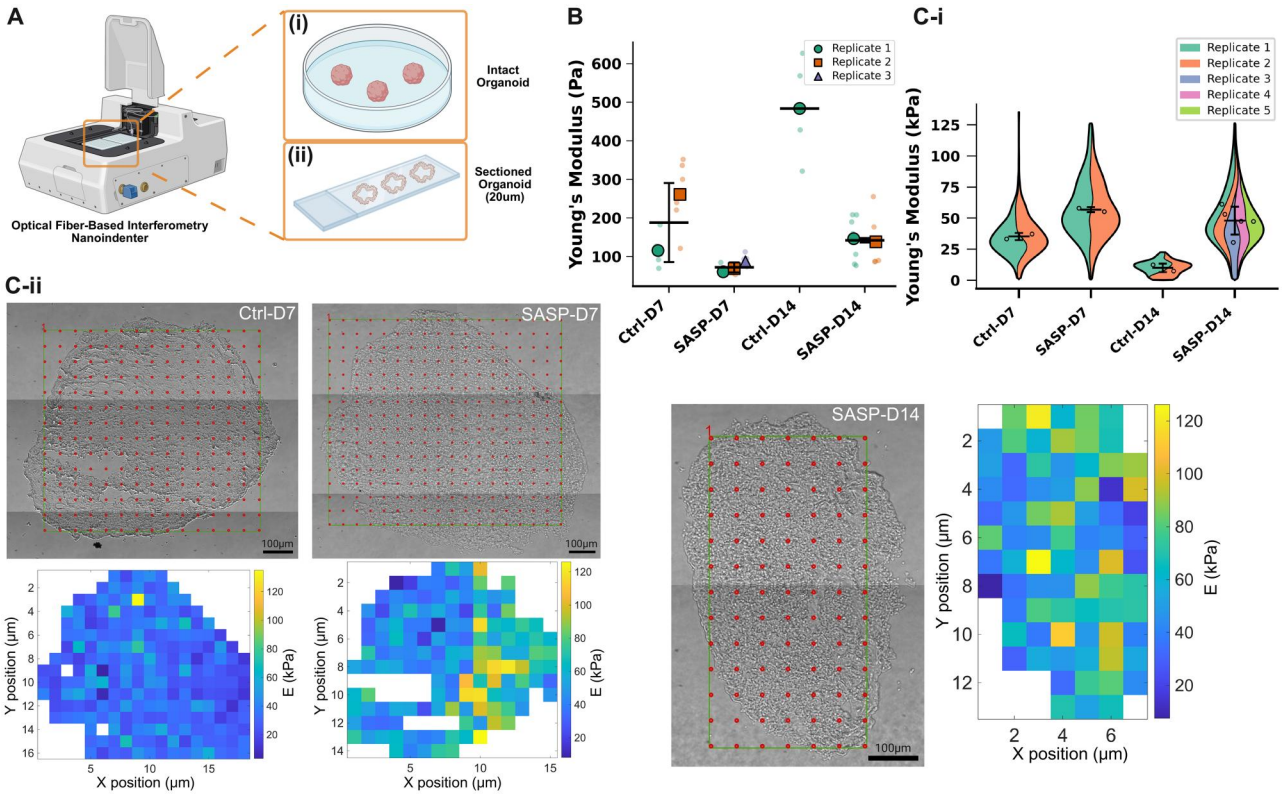


Figure 2. Nanoindentation reveals stiffness heterogeneity in cerebral organoids. (A) Workflow for nanoindentation of (i) live intact organoids and (ii) cryosections. (B) Elastic modulus of live organoids measured by optical fiber interferometric nanoindentation. $n = 2$, 3, 1, and 2 independently measured organoids for Ctrl-D7, SASP-D7, Ctrl-D14, and SASP-D14, respectively. Six to nine indentation positions were averaged to generate one value per organoid; individual indentation positions were not treated as independent experimental replicates. Pale points show individual indentation positions; symbols indicate organoid means; the horizontal line is the mean of organoid means, and error bars are SD across organoids. (C-i) Violin SuperPlots of modulus distributions in cryosections. $n = 2$, 2, 2, and 5 experimental replicates for Ctrl-D7, SASP-D7, Ctrl-D14, and SASP-D14, respectively, with each replicate representing 1 cryosection from an independent organoid. Individual indentation measurements are shown to visualize within-specimen distributions; statistical comparisons were performed using 1 mean value per experimental replicate. (C-ii) Representative spatial stiffness maps of cryosectioned organoids. Grid spacing = 50 μm. Scale bar = 100 μm. A total of 83-406 indentation positions were acquired per condition. Abbreviation: SASP, senescence-associated secretory phenotype. Created in BioRender. Kim, C. (2026) https://BioRender.com/9m772ux

aging.[14] Among 6 samples ($n = 3$ biological replicates per group), 30 605 genes were detected, with 2477 differentially expressed genes (DEGs), including 1700 upregulated and 777 downregulated transcripts.

Unsupervised clustering and functional enrichment analyses revealed that SASP exposure upregulated gene sets associated with ossification, wound healing, vascular remodeling, actin filament bundling, and interleukin signaling, suggesting activation of tissue remodeling and immune-related pathways in brain organoids (Figure 3A). In contrast, downregulated genes were enriched for neurodevelopmental and synaptic processes, including glutamatergic synapse function, dopamine secretion, vesicle transport, and learning and memory pathways, consistent with suppression of neuronal transcriptional activity, synaptic plasticity, and neurotransmission in SASP-treated organoids. Hierarchical clustering further confirmed reproducible transcriptomic shifts across biological replicates following SASP exposure (Figure 3B). Notably, SASP-treated organoids exhibited upregulation of aging-associated neuroinflammation and cognitive dysfunction genes, including IGFBP3, B2M, and SERPINE1[15–17] alongside downregulation of neural developmental genes such as MYT1_1 and MARF1.[18,19] These patterns suggest a mechanistic link between the bone secretome and molecular pathways relevant to brain aging and degeneration. Gene set intersection analysis using Allen Brain Atlas datasets[20,21] revealed overlap between SASP-induced DEGs and established brain aging- and disease-related pathways (Figure 3C).[22,23] Upregulated genes were enriched in NF-κB signaling, inflammation, oxidative stress, and neurodegenerative pathways,[22,24] whereas downregulated genes were associated with GABA receptor signaling. These results indicate that SASP exposure induces transcriptional changes linked to inflammatory activation and neuronal dysfunction seen with aging and disease. Consistent with these findings, Gene Ontology and KEGG pathway enrichment analyses further indicated activation of ECM remodeling, adhesion, and inflammatory signaling pathways, alongside suppression of synaptic and neurotransmission-related processes in SASP-treated organoids (Figure S3, see online supplementary material for a color version of this figure).

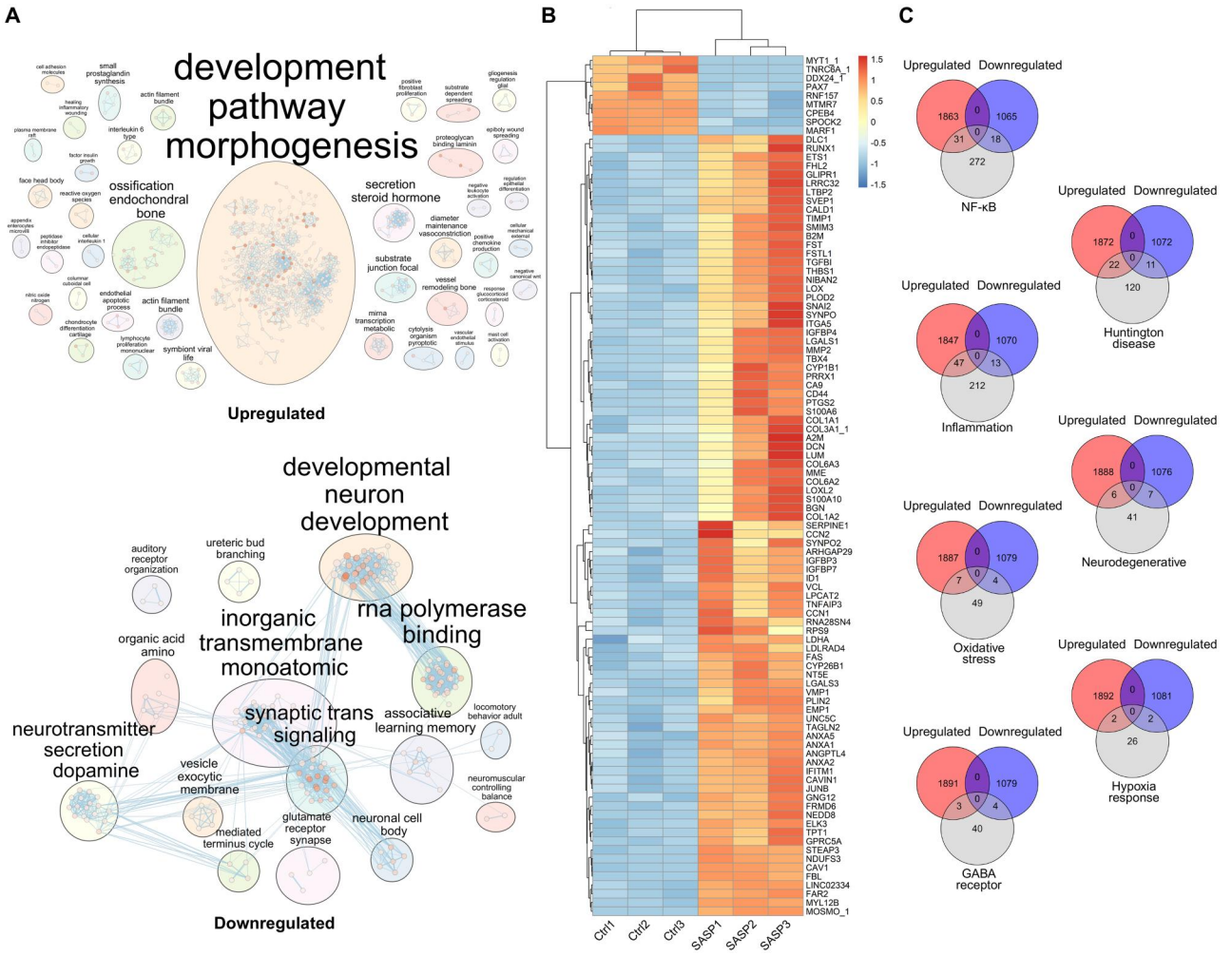


Figure 3. SASP induces inflammatory/ECM pathways and represses synaptic genes. (A) Pathway enrichment of upregulated (top) and downregulated (bottom) genes in SASP-treated organoids. (B) Heatmap of the most significantly differentially expressed genes (adjusted *P*-value). (C) Venn diagrams comparing SASP-regulated genes with Allen Brain Atlas disease and classification datasets. $n = 3$ biological replicates per group. Abbreviation: SASP, senescence-associated secretory phenotype. Created in BioRender. Kim, C. (2026) https://BioRender.com/9m772ux

Activation of pro-inflammatory and senescence-associated markers in cerebral organoids

To spatially assess transcriptomically predicted inflammatory and senescence-associated responses, multiplex immunofluorescence was performed in cerebral organoids after 7 days of bone-derived SASP exposure relative to control (Figure 4). Immunostaining showed altered spatial distribution of IL-1β in SASP-treated organoids, with broader signal localization relative to controls (Figure 4A and B). However, quantitative image analysis did not detect a statistically significant difference in overall IL-1β or IL-6 fluorescence at D7 (Figure 4A-C). In contrast, NF-κB fluorescence was significantly increased following SASP exposure, and p21 signal was also elevated, consistent with activation of inflammatory stress signaling and a senescence-associated response within the organoid microenvironment. Together, these data indicate that early SASP exposure is associated with increased NF-κB and p21 immunoreactivity even in the absence of a statistically significant increase in IL-1β or IL-6 immunofluorescence at this time point. Prolonged exposure to SASP (D14) was associated with broader and stronger signals of IL-1β, IL-6, NF-κB, and p21 relative to controls (Figure S4, see online supplementary material for a color version of this figure), suggesting amplification of inflammatory and senescence-associated signaling over time.[25]

Discussion

Together, our findings suggest that bone-derived SASP senescence-associated secretomes can alter the structural, mechanical, and inflammatory state of human cerebral organoids. Across imaging, nanoindentation, transcriptomic, and immunofluorescence readouts, SASP exposure was associated with localized cytoskeletal irregularity, altered microscale mechanical patterning, induction of extracellular matrix programs, and suppression of synaptic and neurodevelopmental gene networks. At D7, immunofluorescence showed increased NF-κB and p21, whereas IL-1β and IL-6 were not significantly different between groups, indicating an early and selective inflammatory/stress

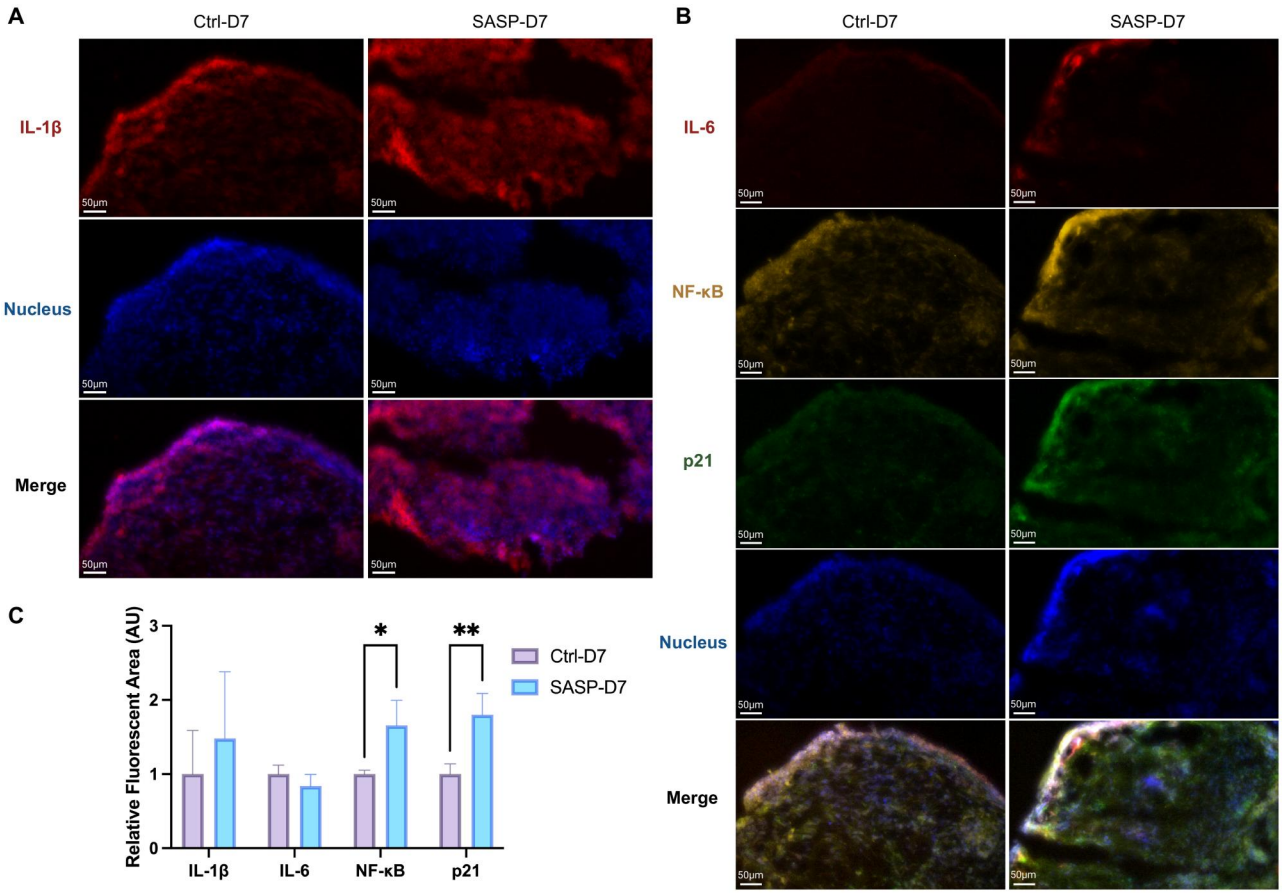


Figure 4. SASP induces inflammatory and senescence markers in cerebral organoids. (A) Immunofluorescence staining of IL-1β and nuclei. (B) Multiplex staining for IL-6, NF-κB, p21, and nuclei. (C) Quantification of fluorescence area for inflammatory/senescence markers (Fiji), normalized to Ctrl-D7. $n = 4$-5 micrographs per condition/time point. Mean ± SD. *$P < .05$, **$P < .01$. Scale bar = 50 μm. Abbreviation: SASP, senescence-associated secretory phenotype. Created in BioRender. Kim, C. (2026) https://BioRender.com/9m772ux

response rather than broad inflammatory activation. Viewed together, these data are consistent with a model in which bone-derived senescence signals may perturb the cerebral microenvironment in a spatially heterogeneous manner. Importantly, we do not interpret altered organoid stiffness as a direct surrogate for cognitive decline. Rather, its co-occurrence with ECM and inflammatory programs and suppression of synaptic and neurodevelopmental pathways supports spatial mechanical heterogeneity as 1 tissue-level feature of a perturbed neural microenvironment.[9] Here, "mechanical vulnerability" refers to altered spatial mechanical organization rather than demonstrated neurological or cognitive impairment.

The translational significance of this study is the introduction of a cross-organ human model for probing bone-to-brain senescence signaling with spatially resolved mechanical readouts. The model is deliberately reductionist and exposes organoids directly to conditioned medium, thereby bypassing the circulation and BBB. It therefore tests whether the senescent osteocyte secretome is sufficient to alter cerebral tissue under direct exposure; it does not establish which secreted factors circulate, cross the BBB, or reach brain parenchyma at biologically relevant concentrations in vivo. Because SASP composition can vary with the senescence-inducing stimulus and cellular context, whether these organoid responses generalize to other models of osteocyte senescence remains to be established. We focused on osteocytes because they are highly abundant, long-lived, terminally differentiated skeletal cells that acquire senescence-associated phenotypes with aging, making them a biologically relevant source of bone-derived senescence signals.[26–28] However, the present single-lineage design does not establish whether the observed cerebral responses are specific to osteocyte-derived SASP or are shared across senescent cell lineages.

While the present work represents a pilot-scale study using a single control iPSC line, the convergence of structural, mechanical, and molecular readouts supports the utility of this system for investigating bone-to-brain senescence signaling. Validation across independent iPSC lines will be required to establish the generalizability of these responses across genetic backgrounds. Next steps will include expansion to patient-matched human systems, including human bone-derived aged or senescence-associated secretomes, autologous iPSC-derived cerebral organoids, and higher-resolution single-cell or single-nucleus multiomic analyses. Together, these advances should enable a deeper mechanistic definition of how peripheral senescence signals remodel the cerebral microenvironment during aging, shedding light on potential age-related degenerative processes within the bone-brain axis.

Senescence-associated secretory phenotype-mediated paracrine effects can extend across distinct cell lineages; for example, secretome from senescent mesenchymal stromal cells altered the growth of prostate epithelial cells in a recipient cell-dependent manner.[29] Senescence-associated phenotypes have also been described in neural cells, including following reduced MECP2 expression, which perturbs neural cell commitment and neuronal maintenance.[30] These studies provide relevant context for cross-lineage senescence signaling, although the present study did not establish senescence specifically within neurons.

Conclusion

Bone-derived senescence-associated secretomes are associated with structural, mechanical, and early inflammatory and senescence-associated changes in human cerebral organoids. Senescence-associated secretory phenotype exposure was associated with localized cytoskeletal alterations, altered microscale mechanical patterning, and inflammatory and extracellular matrix pathway changes. These findings position tissue mechanics as a candidate readout of bone-brain crosstalk and the senescent bone secretome as a candidate contributor to neural microenvironmental vulnerability in aging. These pilot-scale observations were obtained using a single iPSC line and a single conditioned-medium batch, with 1-6 experimental replicates per condition across assays. Thus, future studies incorporating independent iPSC lines, independently generated SASP-CM batches, and larger experimental replication will be needed to establish the reproducibility and generalizability of these findings.

Acknowledgments

Figure schematics and assemblies of quantified and analyzed data were done with a BioRender.com license to BioMATTER Lab (Tilton group). Bulk RNA sequencing was performed by 7-Traits Genomics through a service contract. The authors also acknowledge support from the core facilities at The University of Texas at Austin.

Supplementary material

Supplementary material is available at *Stem Cells* online.

Funding

This work was supported by startup funds to M.T. from the Walker Department of Mechanical Engineering at The University of Texas at Austin and to A.K. from the Department of Biomedical Engineering at Johns Hopkins University, as well as by the National Institute on Aging of the National Institutes of Health (NIH) (K25AG095370 to M.T.), the Maryland Stem Cell Research Fund (to A.K.), and NIH grant R37AG013925 (to J.L.K.).

Conflicts of interest

The authors declare no conflicts of interest.

Data availability

The data underlying this article will be shared on reasonable request to the corresponding authors.

References

1. Wanionok NE, Morel GR, Fernández JM. Osteoporosis and Alzheimer's disease (or Alzheimer's disease and osteoporosis). *Ageing Res Rev*. 2024;99:102408. https://doi.org/10.1016/j.arr.2024.102408
2. Ogunwale AN, Schulz PE, Des Bordes JK, Elefteriou F, Rianon NJ. Potential biological and genetic links between dementia and osteoporosis: a scoping review. *Geriatrics (Basel)*. 2025;10:96. https://doi.org/10.3390/geriatrics10040096
3. Guerrero A, De Strooper B, Arancibia-Cárcamo IL. Cellular senescence at the crossroads of inflammation and Alzheimer's disease. *Trends Neurosci*. 2021;44:714-727. https://doi.org/10.1016/j.tins.2021.06.007
4. Farr JN, Khosla S. Cellular senescence in bone. *Bone*. 2019;121:121-133. https://doi.org/10.1016/j.bone.2019.01.015
5. Knopp RC, Erickson MA, Rhea EM, Reed MJ, Banks WA. Cellular senescence and the blood-brain barrier: implications for aging and age-related diseases. *Exp Biol Med (Maywood)*. 2023;248:399-411. https://doi.org/10.1177/15353702231157917
6. Shi T, Shen S, Shi Y, et al. Osteocyte-derived sclerostin impairs cognitive function during ageing and Alzheimer's disease progression. *Nat Metab*. 2024;6:531-549. https://doi.org/10.1038/s42255-024-00989-x
7. Das MM, Godoy M, Chen S, et al. Young bone marrow transplantation preserves learning and memory in old mice. *Commun Biol*. 2019;2:73. https://doi.org/10.1038/s42003-019-0298-5
8. Khrimian L, Obri A, Ramos-Brossier M, et al. Gpr158 mediates osteocalcin's regulation of cognition. *J Exp Med*. 2017;214:2859-2873. https://doi.org/10.1084/jem.20171320
9. Hall CM, Moeendarbary E, Sheridan GK. Mechanobiology of the brain in ageing and Alzheimer's disease. *Eur J Neurosci*. 2021;53:3851-3878. https://doi.org/10.1111/ejn.14766
10. Tilton M, Liao J, Kim C, et al. Tracing cellular senescence in bone: time-dependent changes in osteocyte cytoskeleton mechanics and morphology. *Small*. 2025;21:e2408517. https://doi.org/10.1002/smll.202408517
11. Tilton M, Weivoda M, Astudillo Potes M, et al. Stiffening symphony of aging: biophysical changes in senescent osteocytes. *Aging Cell*. 2024;23:e14421. https://doi.org/10.1111/acel.14421
12. Dimitriadis EK, Horkay F, Maresca J, Kachar B, Chadwick RS. Determination of elastic moduli of thin layers of soft material using the atomic force microscope. *Biophys J*. 2002;82:2798-2810. https://doi.org/10.1016/S0006-3495(02)75620-8
13. Li X, Li C, Zhang W, Wang Y, Qian P, Huang H. Inflammation and aging: signaling pathways and intervention therapies.

Signal Transduct Target Ther. 2023;8:239. https://doi.org/10.1038/s41392-023-01502-8
14. Chinta SJ, Woods G, Rane A, Demaria M, Campisi J, Andersen JK. Cellular senescence and the aging brain. *Exp Gerontol*. 2015;68:3-7. https://doi.org/10.1016/j.exger.2014.09.018
15. Salzmann A, James SN, Williams DM, et al. Investigating the relationship between IGF-I, IGF-II, and IGFBP-3 concentrations and later-life cognition and brain volume. *J Clin Endocrinol Metab*. 2021;106:1617-1629. https://doi.org/10.1210/clinem/dgab121
16. Zhong Q, Zou Y, Liu H, et al. Toll-like receptor 4 deficiency ameliorates β2-microglobulin induced age-related cognition decline due to neuroinflammation in mice. *Mol Brain*. 2020;13:20. https://doi.org/10.1186/s13041-020-0559-8
17. Kutz SM, Higgins CE, Higgins PJ. Novel combinatorial therapeutic targeting of PAI-1 (SERPINE1) gene expression in Alzheimer's disease. *Mol Med Ther*. 2012;1:106. https://doi.org/10.4172/2324-8769.1000106
18. Chen J, Yen A, Florian CP, Dougherty JD. MYT1L in the making: emerging insights on functions of a neurodevelopmental disorder gene. *Transl Psychiatry*. 2022;12:292. https://doi.org/10.1038/s41398-022-02058-x
19. Kanemitsu Y, Fujitani M, Fujita Y, et al. The RNA-binding protein MARF1 promotes cortical neurogenesis through its RNase activity domain. *Sci Rep*. 2017;7:1155. https://doi.org/10.1038/s41598-017-01317-y
20. Lein ES, Hawrylycz MJ, Ao N, et al. Genome-wide atlas of gene expression in the adult mouse brain. *Nature*. 2007;445:168-176. https://doi.org/10.1038/nature05453
21. Allen Institute for Brain Science. Allen mouse brain atlas. 2004. Accessed March 2, 2026. https://mouse.brain-map.org
22. Xu J, Zhou H, Xiang G. Identification of key biomarkers and pathways for maintaining cognitively normal brain aging based on integrated bioinformatics analysis. *Front Aging Neurosci*. 2022;14:833402. https://doi.org/10.3389/fnagi.2022.833402
23. Su X, Xie L, Li J, Tian X, Lin B, Chen M. Exploring molecular signatures related to the mechanism of aging in different brain regions by integrated bioinformatics. *Front Mol Neurosci*. 2023;16:1133106. https://doi.org/10.3389/fnmol.2023.1133106
24. Primiani CT, Ryan VH, Rao JS, et al. Coordinated gene expression of neuroinflammatory and cell signaling markers in dorsolateral prefrontal cortex during human brain development and aging. *PLoS One*. 2014;9:e110972. https://doi.org/10.1371/journal.pone.0110972
25. Malaquin N, Martinez A, Rodier F. Keeping the senescence secretome under control: molecular reins on the senescence-associated secretory phenotype. *Exp Gerontol*. 2016;82:39-49. https://doi.org/10.1016/j.exger.2016.05.010
26. Farr JN, Fraser DG, Wang H, et al. Identification of senescent cells in the bone microenvironment. *J Bone Miner Res*. 2016;31:1920-1929. https://doi.org/10.1002/jbmr.2892
27. Farr JN, Xu M, Weivoda MM, et al. Targeting cellular senescence prevents age-related bone loss in mice. *Nat Med*. 2017;23:1072-1079. https://doi.org/10.1038/nm.4385
28. Farr JN, Saul D, Doolittle ML, et al. Local senolysis in aged mice only partially replicates the benefits of systemic senolysis. *J Clin Invest*. 2023;133:e162519. https://doi.org/10.1172/JCI162519
29. Alessio N, Aprile D, Squillaro T, et al. The senescence-associated secretory phenotype (SASP) from mesenchymal stromal cells impairs growth of immortalized prostate cells but has no effect on metastatic prostatic cancer cells. *Aging (Albany NY)*. 2019;11:5817-5828. https://doi.org/10.18632/aging.102172
30. Squillaro T, Alessio N, Cipollaro M, et al. Reduced expression of MECP2 affects cell commitment and maintenance in neurons by triggering senescence: new perspective for Rett syndrome. *Mol Biol Cell*. 2012;23:1435-1445. https://doi.org/10.1091/mbc.E11-09-0784

© The Author(s) 2026. Published by Oxford University Press.

This is an Open Access article distributed under the terms of the Creative Commons Attribution-NonCommercial License (https://creativecommons.org/licenses/by-nc/4.0/), which permits non-commercial re-use, distribution, and reproduction in any medium, provided the original work is properly cited. For commercial re-use, please contact reprints@oup.com for reprints and translation rights for reprints. All other permissions can be obtained through our RightsLink service via the Permissions link on the article page on our site—for further information please contact journals.permissions@oup.com.
Stem Cells, 2026, 44, 1–9
https://doi.org/10.1093/stmcls/sxag057
Brief Report